

We are IntechOpen, the world's leading publisher of Open Access books Built by scientists, for scientists

4,800

Open access books available

122,000

International authors and editors

135M

Downloads

Our authors are among the

154

Countries delivered to

TOP 1%

most cited scientists

12.2%

Contributors from top 500 universities



WEB OF SCIENCE™

Selection of our books indexed in the Book Citation Index
in Web of Science™ Core Collection (BKCI)

Interested in publishing with us?
Contact book.department@intechopen.com

Numbers displayed above are based on latest data collected.
For more information visit www.intechopen.com



Nanotechnology and Development of Strain Sensor for Damage Detection

Yumna Qureshi, Mostapha Tarfaoui, Khalil K. Lafdi and Khalid Lafdi

Abstract

Composite materials, having better properties than traditional materials, are susceptible to potential damage during operating conditions, and this issue is usually not found until it is too late. Thus, it is important to identify when cracks occur within a structure, to avoid catastrophic failure. The objective of this chapter is to fabricate a new generation of strain sensors in the form of a wire/thread that can be incorporated into a material to detect damage before they become fatal. This microscale strain sensor consists of flexible, untwisted nylon yarn coated with a thin layer of silver using electroless plating process. The electromechanical response of this sensor wire was tested experimentally using tensile loading and then verified numerically with good agreement in results. This flexible strain sensor was then incorporated into a composite specimen to demonstrate the detection of damage initiation before the deformation of structure becomes fatal. The specimens were tested mechanically in a standard tensometer machine, while the electrical response was recorded. The results were very encouraging, and the signal from the sensor was correlated perfectly with the mechanical behavior of the specimen. This showed that these flexible strain sensors can be used for in situ structural health monitoring (SHM) and real-time damage detection applications.

Keywords: composites, structural health monitoring, flexible yarn, strain sensor, conductive film Ag-coating, electromechanical behavior

1. Introduction

Composite materials, despite having better physical properties, are not exempt from limitations and drawbacks [1–4]. The mechanisms of damage initiation and propagation leading to ultimate fracture in these materials are very complex but very well established [5–11]. Structural health monitoring (SHM) is a well-known technique to examine the mechanical behavior of the structure during operation and to avoid its sudden failure [12]. In situ real-time SHM has been used frequently for detecting different types of damages in materials such as corrosion, deformation, debonding/delamination, fiber cracking, thermal degradation, intralaminar cracking, etc. to ensure safe and durable service life of the structures [13–18]. So, vast research had been carried out during the past years to develop SHM sensors, and this development took place gradually over time from strain gages, fiber optic

sensors, and piezoelectric sensors to microelectromechanical systems (MEMSs) [19–21]. But they all have some limitations such as strain gauges behave as defects or inclusions, fiber optic sensors require lot of instrumentation and data analysis, brittle material is used in manufacturing piezoelectric sensors, and MEMSs are manufactured at microscale, which makes the manufacturing process difficult [22–25].

Another class of sensors, known as textile sensors or flexible sensors, is the new focus of study for many researchers. These are conductive strain sensor wires/threads in which electrical resistance varies reversibly to applied stress [26–29]. They can be developed at nanoscale or microscale and can overcome the limitation of brittle behavior of conventional piezo-resistive strain gauges. So, it is essential to understand the mechanical behavior of these flexible sensors for better structural integrity and longer service life. Moreover, it is also important to understand the concept of computational modeling of these flexible yarns to model and analyze their behavior numerically. However, very less research has been conducted to use the concept of coated yarn as a flexible piezo-resistive strain sensor for structural health monitoring without jeopardizing the mechanical behavior of core material especially numerically. Different researchers had worked on numerical models and had used finite element analysis (FEA) to predict the mechanical behavior of yarn [30–32]. With the advancement of computer-aided design (CAD) and computer-aided engineering (CAE), it is possible to investigate the mechanical behavior of yarn using finite element modeling (FEM) [33]. Many CAD models of filaments, yarns, and fabrics have been developed by researchers with most of them related to geometrical modeling of yarns based on single line yarn path also known as pitch length [34–37]. Some researchers have attempted to overcome difficulties like small- and large-scale deformation, complex material properties, and 3D modeling [38]. Several analytical models had been established for the estimation of mechanical tensile performance of yarns. The tensile behavior of yarn, using force method, was first studied 90 years ago, which was then extended to examine the mechanical behavior of continuous filament yarns [39, 40]. Other than force method, energy method was used to study the continuous filament and to predict the whole stress-strain behavior in Tenasco yarn which was first proposed by Treloar and Riding [41]. Then, Riding and Wilson [42] extended this study and predicted the stress-strain relations for materials such as low-tenacity Terylene, Super Tenasco, and Nylon 6-6. Moreover, energy method was also used to study the tensile and torsional behavior of bulky wool single yarn [43]. Cartraud and Messenger [44] studied the model of 1 + 6 (six cylindrical filaments were wrapped around a straight filament at core) stranded fibrous structure under tensile loading. Vassiliadis et al. [38] suggested a computational method to study the mechanical behavior of multifilament twisted yarn from 2 to 1200 filaments based on FEM. However, up to this date and to the best knowledge of the author, very limited or no research has been conducted to experimentally and/or numerically analyze a coated yarn and to study the electromechanical response of coated yarn-based wire models.

In this chapter, the overall objective is to fabricate a conductive wire that functions like a piezo-resistive strain gage while not jeopardizing the structural integrity of the composite and acting as a real-time sensor during the operating condition. This was achieved by using untwisted nylon yarn and depositing silver metal coating on its surface. Initially, experimental tests were conducted to quantify the electromechanical behavior of this detector and analyze its performance. Then, a numerical model was developed to validate this sensor design and confirm the reproducibility of results. Due to their extremely small size and large-scale integration degree, the sensors had the remarkable characteristics of light weight, flexibility in design, low power consumption and noise level, short response time, high

reliability, and low cost. Once the experimental results were validated numerically, these microscale flexible sensor wires were incorporated in the composite specimen to demonstrate its SHM application. The specimens were then tested in standard tensometer machine mechanically while the electrical response was recorded, which correlated perfectly with the mechanical behavior of composite specimen. This showed that these flexible yarn wires can be used as piezo-resistive strain sensors for SHM applications of composite structures.

2. Sensor fabrication and characterization

Sensors were developed using untwisted nylon yarn and by depositing a silver (Ag) metal film on the surface of its filaments because even though nylon yarn behaved well mechanically, it was poor in electrical conductance. Thin film coating was applied to overcome the conductance issue without jeopardizing structural integrity of each material. Electroless plating process was used for this purpose, and the sensor specimens were characterized by the following dimensions: length 50 mm, diameter of yarn 225 μm , and coating thickness 1–2 μm . This thickness of the coating film is the best compromise between uniform thickness throughout the yarn and good conductive flexible coating. These dimensions were confirmed when scanning electron microscopy (SEM) of sample wires was performed for the characterization of samples after deposition of silver coating.

3. Experimental test setup for sensor wires

Uniaxial tensile testing machine and oscilloscope were used simultaneously to examine the sensing behavior of this flexible strain sensor wire. Three experimental

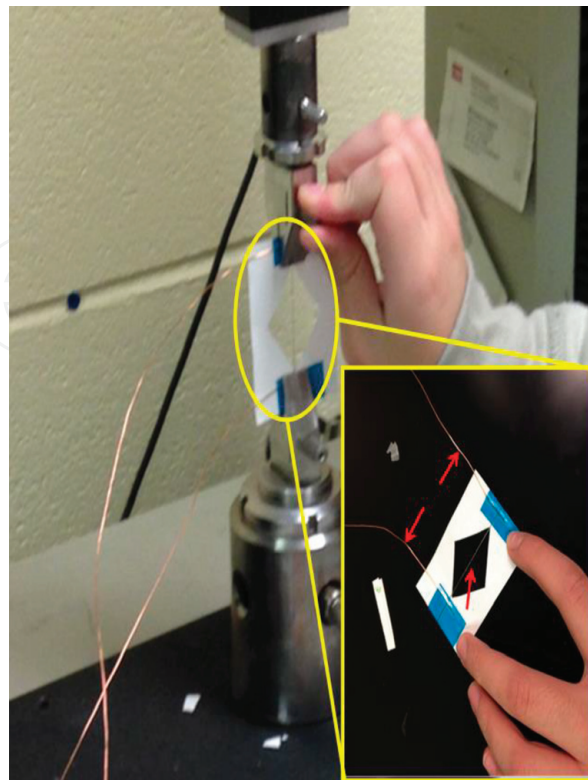


Figure 1.
Flexible sensor wire was attached with electrodes and paper support, placed in the tensile machine, and electrodes were attached to the data acquisition system.

tests were performed to confirm the reproducibility of the results. Paper frame was used specifically to provide support to such a small specimen in the tensile machine; however, it was cut from the sides before starting the test so it could not affect the behavior of sensor during the test. In addition, electrodes were attached at both ends of the specimen to provide better connection. Then, the specimen was placed in the tensile machine and test was performed at low strain rate, that is 5 mm/min, **Figure 1**. As a result, the stress-strain behavior with resistance profile was obtained.

4. Numerical modeling of sensor wire

Coupled field analysis in commercial Abaqus/standard software was used to model the electromechanical behavior and verify experimental results. The sample geometry of conductive thin film-coated monofilament was developed at the microscale to avoid aspect ratio problems during meshing and reduce the computational time, **Figure 2a** and **b**. Before performing the finite element analysis, it was

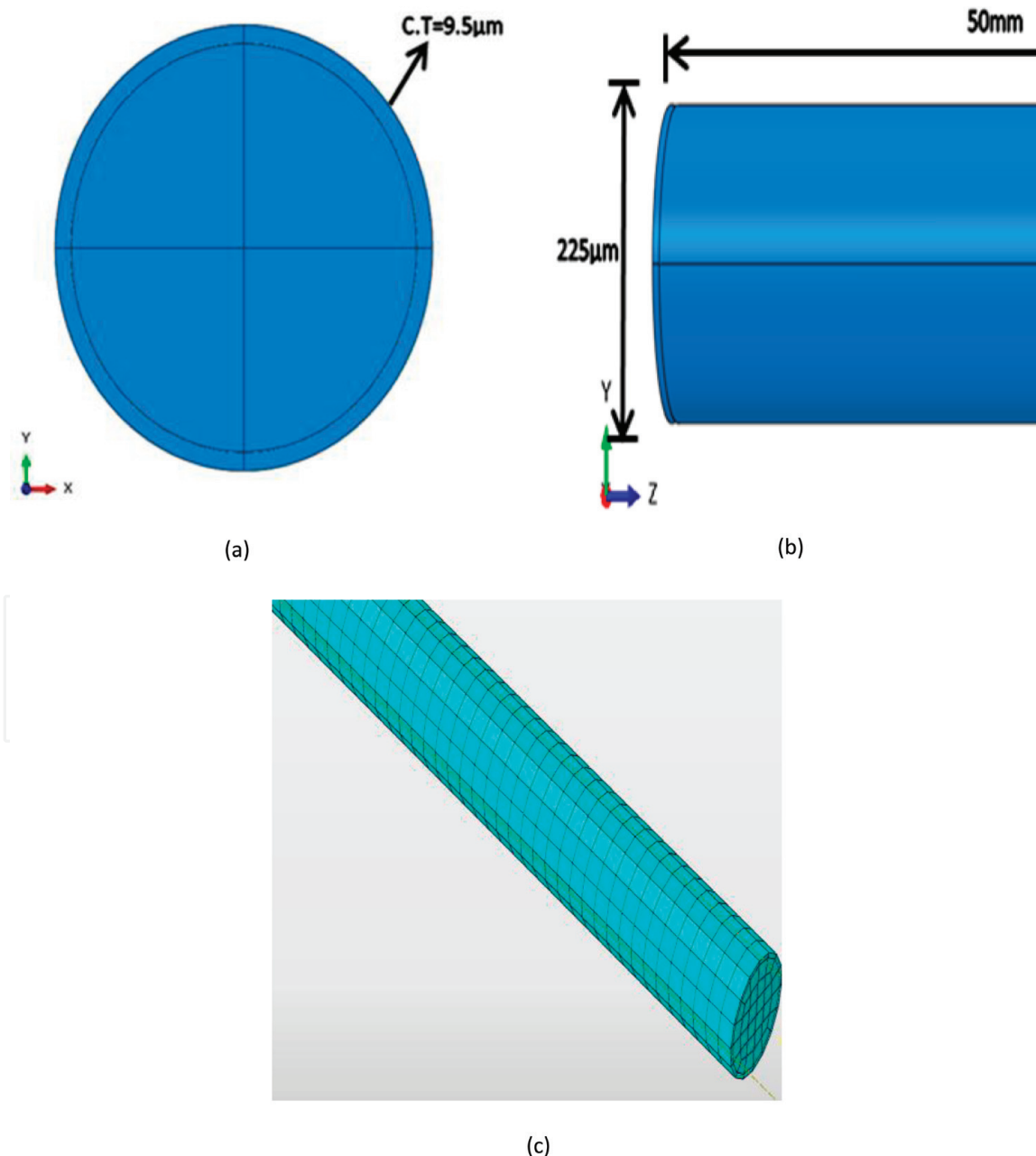


Figure 2. Schematic representation of the coated yarn: (a) front view, (b) side view, and (c) mesh of the yarn.

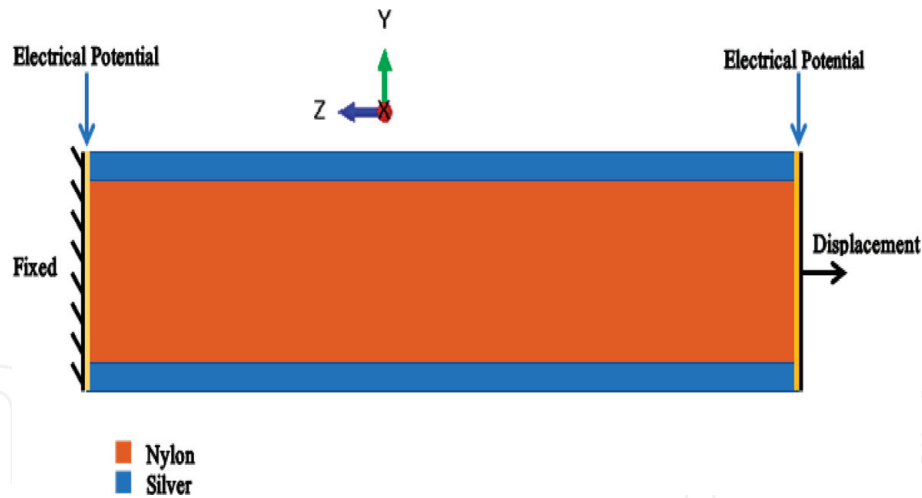


Figure 3.
Electromechanical boundary conditions applied to the 3D model.

important to ensure the convergence of the mesh. So, mesh convergence study was performed on the model to eliminate the dependency upon the mesh for which 5 mesh sizes, 1, 0.5, 0.1, 0.08, and 0.05 were considered, and, based on the study, mesh size 0.05 was used for discrete model because it was the best compromise between less computational work and accuracy of results, **Figure 2c**. The applied boundary conditions consisted of both mechanical and electrical loads, **Figure 3**.

5. Fabrication of composite specimens incorporated with sensor

Standard specimens of composites for tensile test were prepared and a full integration of sensors into the composite structure was achieved, **Figure 4**. Silicon

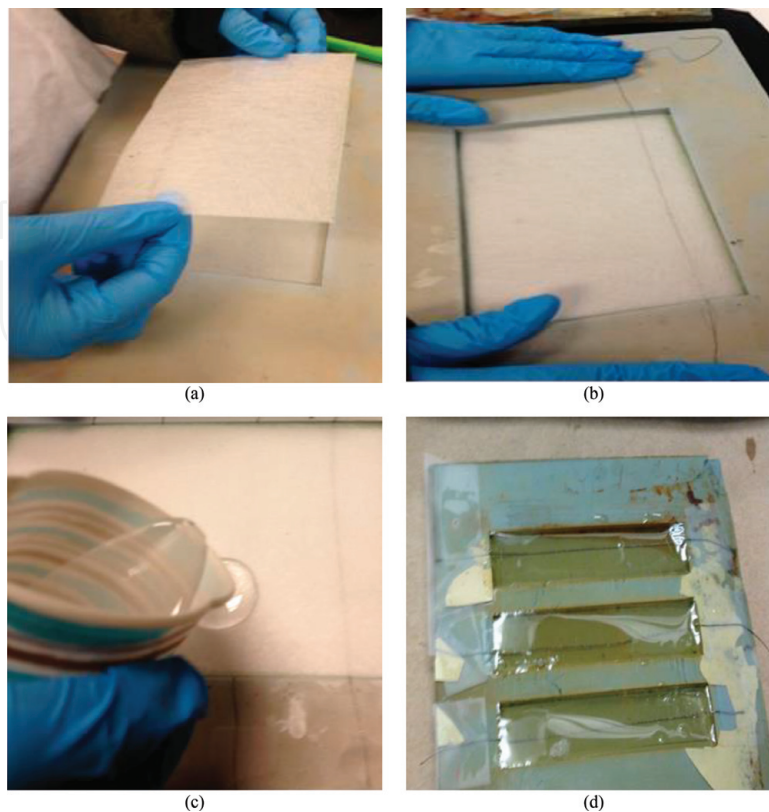


Figure 4.
Fabrication of composite specimen with sensor wire.

molds were used for the preparation of samples and glass fiber fabric was used as reinforcement. The glass fabric was cut into segments and placed into a mold and a sensor (nylon yarn coated with silver) was inserted between the plies of fiberglass. Then, resin mixed with hardener with a ratio of 1:4 was poured into the mold. Once the molds were filled, one could no longer see the fiberglass layers, the samples were completely transparent. Now, one could view all of the sensors easily. After that, samples were left to cure for 48 hours at room temperature.

6. Experimental test of composite with sensor wire

A cured composite sample with integrated sensor was tested using an Instron test machine and the oscilloscope was connected to sensor lids. Uniaxial tensile testing machine and oscilloscope were used simultaneously to correlate the mechanical behavior of the composite specimen with the electrical response of the strain sensor wire. Three experimental tests were performed to confirm the reproducibility of the results. In addition, electrodes were attached at both ends of the specimen to provide better connection. Then, the specimen was placed in the tensile machine and test was performed, **Figure 5**. As a result, the stress-strain behavior of composite specimen with resistance profile of the sensor was obtained.

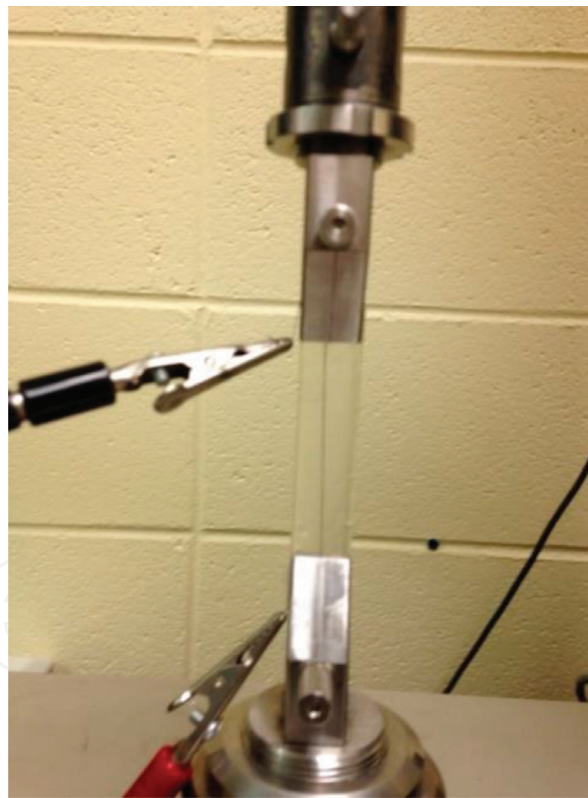


Figure 5.
Composite sample mounted on test frame for mechanical test. Sensor lids are connected to the oscilloscope.

7. Results and discussion

7.1 SEM characterization of flexible strain sensor wires

All the filaments were uniformly coated; however, after large magnification, it appeared that some filaments exhibited cracks or gaps. Another phenomenon observed during the SEM characterization was that the silver coating was made of

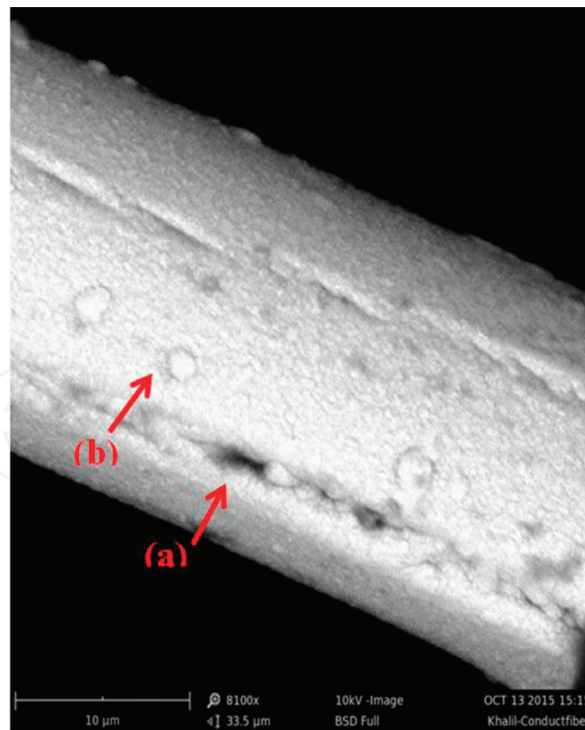


Figure 6. SEM characterization of the Ag thin film-coated untwisted yarn: (a) shows the uniform coating with some minute discontinuities and defects in the coating and (b) confirms that the Ag thin film coating on the nylon surface consisted of deposition of nanoparticles of silver.

nanoparticle grains, or aggregates less than one micro-meter in size, **Figure 6**. SEM characterization of the coated untwisted yarn showed uniform coating with some minute discontinuities and defects and also confirmed that the Ag thin film coating consisted of deposition of nanoparticles of silver. Regardless of the imperfections in the Ag film coating in some filaments, it did not seem to affect the electrical conductivity.

7.2. Experimental testing

7.2.1 Electromechanical response

Three tensile tests of piezo-resistive sensor wire were performed. The Young modulus and yield strength of the tested samples were about 1348.5 and 20.13 MPa, respectively. The stress-strain behavior of untwisted coated yarn is shown in **Figure 7a**. Stress and electrical response of the untwisted yarn are plotted simultaneously in **Figure 7b**. The resistance was changed at the same time as the failure started to initiate, and, as the test progressed, the resistance increased gradually when the number of fractured filaments was increased. Ultimately, when the untwisted yarn was fractured completely, the resistance went to maximum value. The results were very encouraging, and piezo-resistive flexible sensor was responding very well to any change in load.

7.2.2 Damage modes

After tensile test, fractured samples were studied using SEM technique, and it appeared that there were two distinct morphologies. Some filaments exhibited a clean ductile failure in which both the coating and the fiber showed a clean cut; however, other filaments showed a pull-out of the coating or flaking off, **Figure 8**.

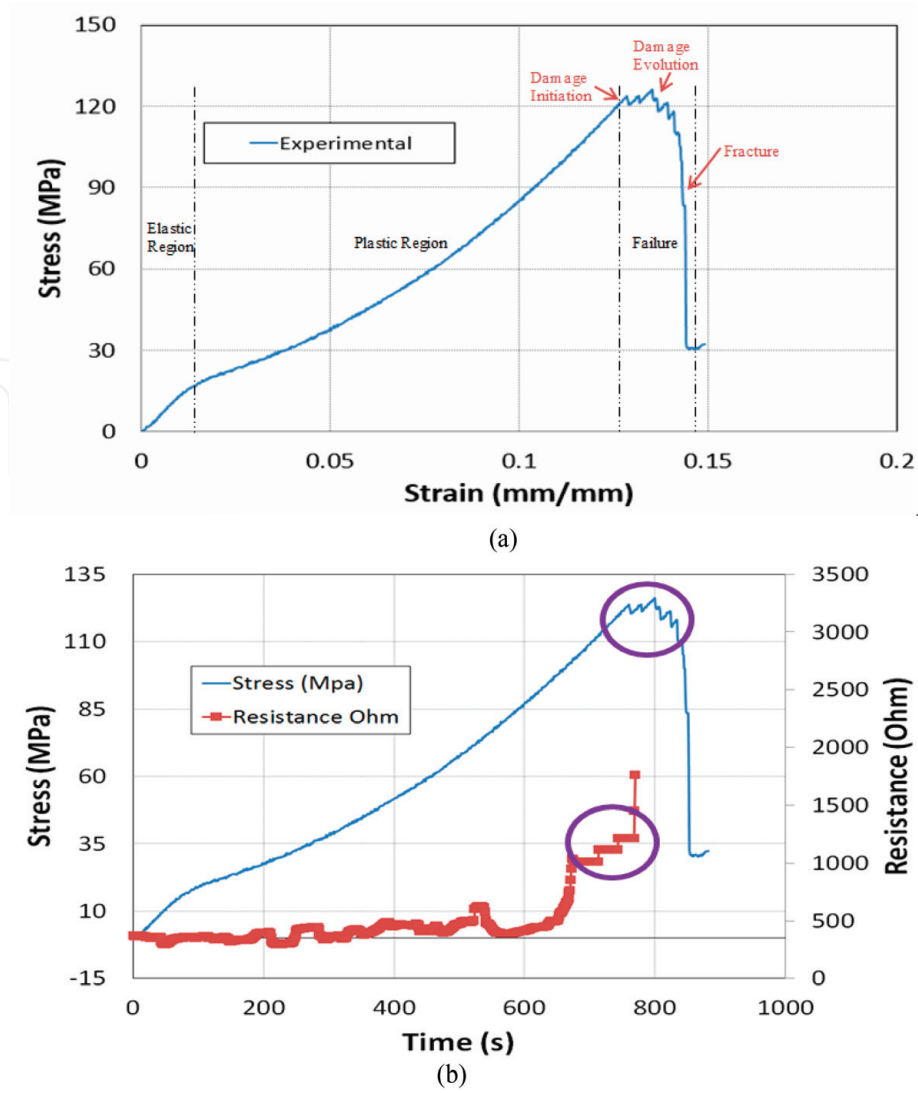


Figure 7. Electromechanical behavior of untwisted nylon yarn: (a) mechanical behavior of untwisted nylon yarn and (b) electromechanical response.

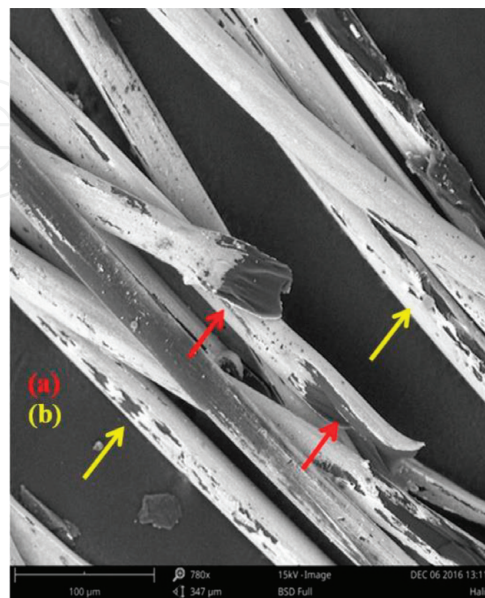


Figure 8. SEM characterization of fractured samples confirms that the coating thickness was approximately 1–2 μm: (a) shows a clear ductile failure of both core and coating material and (b) depicts the second phenomenon, that is, flaking off of coating.

This established that some parts of the coating might not have developed strong adherence with the nylon fiber during the fabrication process. However, it did not affect the overall response of the sensor because of two reasons: first, the pull-out of coating happened during damage initiation and damage propagation just before the failure and did not affect the performance of the sensor before that; the second reason is that there were approximately 100 fibers in the single yarn and fiber pull-out happened in less than 5–10% of fibers, which is almost negligible. Nevertheless, the surface adhesion can be improved during the fabrication process by further improving the surface roughness by etching process before application of coating because rough surfaces have better adhesion properties.

7.3 FE analysis

The untwisted coated yarn was modeled as a ductile material using the built-in elastic, plastic, and ductile damage criteria of Abaqus because both silver and nylon are ductile in nature. Electrical conductance of both materials nylon and Ag thin film was defined in Abaqus to model the electrical response during the mechanical analysis, **Table 1**. For the numerical analysis, experimental tensile behavior of pure silver thin film was applied [45] in addition to the mechanical response of untwisted nylon yarn, **Table 1**.

Furthermore, the rate-dependent power law was defined using the experimental curves in the plasticity model because it plays a vital role in damage initiation and neck formation during ductile failure. Therefore, strain hardening stress coefficient K and strain hardening index n were calculated using Eqs. (1) and (2).

$$n = \frac{\log \sigma_2 - \log \sigma_1}{\log \varepsilon_2 - \log \varepsilon_1} \quad (1)$$

$$\log K - \log \sigma_1 = n(\log x - \log \varepsilon_1) \quad (2)$$

where $\sigma_{1,2}$ are stress points in the plastic region, $\varepsilon_{1,2}$ are the corresponding strain points in the plastic region, K is the strain hardening stress, and n is the strain hardening exponent.

Ductile damage criteria built in Abaqus was used to define model failure. Damage initiation depended on fracture strain, strain rate, and stress triaxiality whereas damage evolution required displacement at failure, **Table 1**. The evolution of the damage defined the material's behavior by illustrating the degradation of material stiffness after damage initiation. Scalar damage approach was used for formulating the rate of damage as given in (3). D is the overall damage variable showing the combined effect of all active damage mechanisms, and when it reached 1, fracture occurred.

$$\sigma = (1 - D) \sigma \quad (3)$$

Material	Electrical conductance, S/mm	Young's modulus, MPa	Poisson ratio	Yield strength, MPa	Fracture strain	Strain rate, mm/min
Nylon	1×10^{-15}	1348.5	0.39	20.13	0.12	5
Silver	63×10^3	47,230	0.37	431.1	0.08	60×10^{-5}

Table 1.
 Experimental elastic, plastic, and failure data of nylon and pure Ag-thin film.

where σ is the stress due to damage response, D is the damage variable, and σ' is the stress due to undamaged response.

7.4 Verification of sensor response

The nylon monofilament coated with silver thin film was subjected to tensile elongation until failure. Results showed that it was viable to use one filament to validate the piezo-resistive behavior of untwisted coated yarn. The true stress-strain behavior showed a good correlation with the experimental results in the elastic-plastic region, **Figure 9**. It can be seen in the results that it was fine to use coated monofilament model to verify the result because the plane of stress is same. However, there is a slight difference in the failure initiation and breakage, which is understandable because: in experimental results, the failure shows gradual breakage of all the monofilaments, whereas in the numerical model, the set of monofilaments is modeled by a single thread. Electrical response was recorded as electrical current density (ECD) in Abaqus which was then converted to resistance response using Eqs. (4)-(6) to validate the experimental piezo-resistive behavior of sensor wire. Electromechanical behavior of the monofilament is shown in **Figure 10**.

$$J = \alpha E \text{ with } \alpha = \frac{1}{\rho} \quad (4)$$

$$J = \frac{E}{\rho} \Rightarrow J \propto \frac{1}{\rho} \quad (5)$$

$$R = \frac{\rho L}{A} \quad (6)$$

where J is the current density, E is the electric field, α is the electrical conductivity, ρ is the resistivity, L is the length, A is the cross-sectional area, and R is the resistance.

It was observed that till the plastic region, the electrical resistivity of the yarn changed, but this change in resistance was very small as compared to change in resistance on damage when there was complete breakage in current flow. No gradual increase in the resistance was seen like in experimental results because of the monofilament model. The 3D discrete model of coated monofilament before and after failure is shown in **Figure 11**.

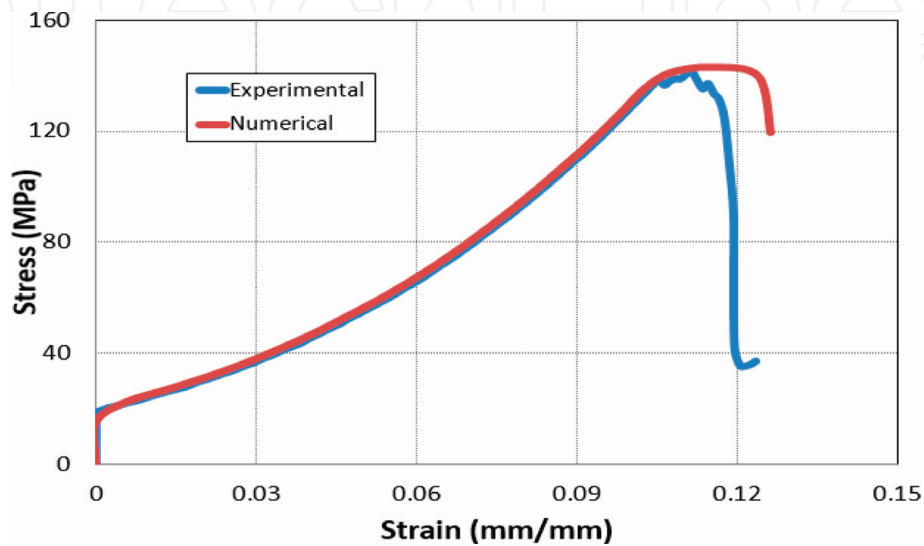


Figure 9. Numerical verification of experimental mechanical behavior of Ag-coated untwisted nylon yarn.

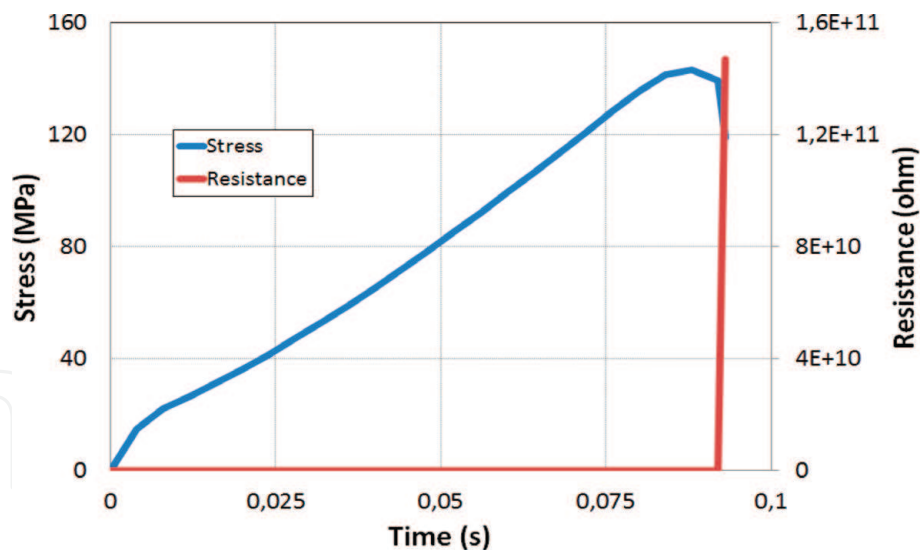


Figure 10.
FE analysis of electromechanical response of Ag-coated monofilament.

7.5 Experimental results of instrumented composite specimen with nylon/silver sensor

Three tensile tests were performed with the composite specimen incorporated with sensor wire. The mechanical response including Young's modulus and yield strength of the tested samples showed that it was not affected by insertion of sensor in the sample and the sensor did not act as intrusive element. The mechanical response of composite specimen and electrical response of the sensor were correlated simultaneously. The resistance was changed at the same time as the failure started to initiate, and, as the test progressed, at the point of failure, the resistance of the sensor started to increase and eventually went to infinity, **Figure 12**. The sensor was reporting what was going on as the fracture formed. The results were

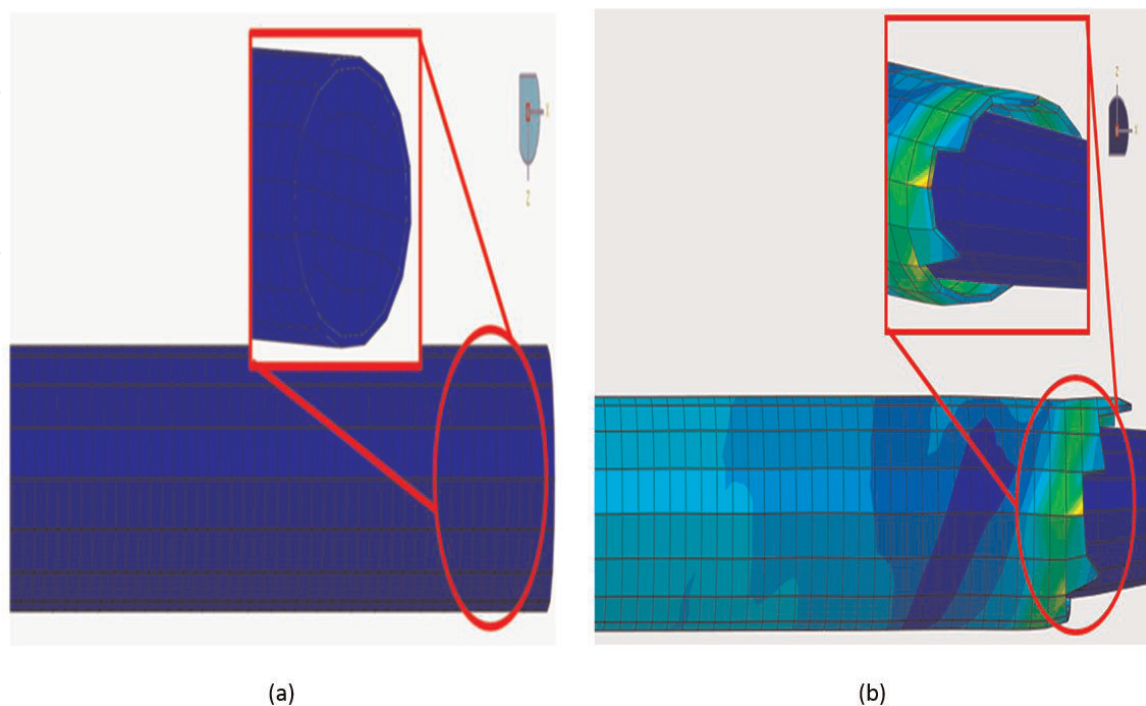


Figure 11.
3D discrete model (a) before failure and (b) after failure.

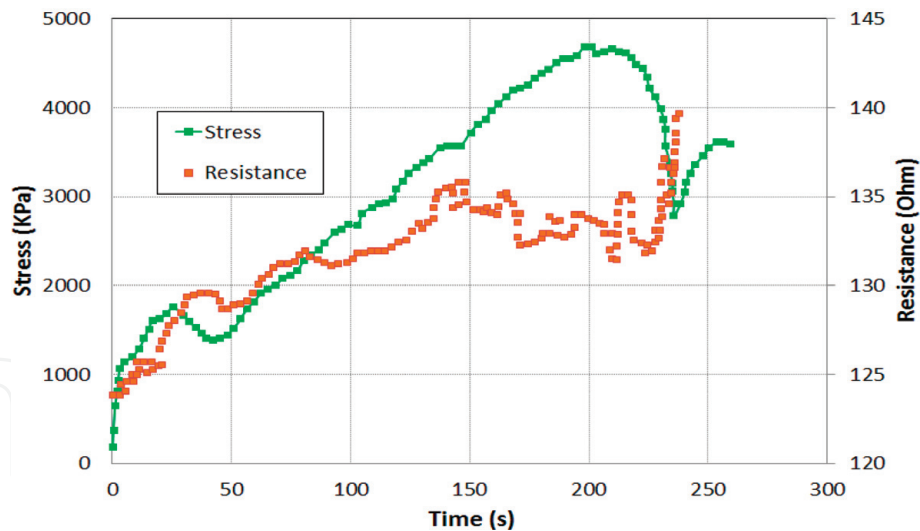


Figure 12.
Electrical response of the sensor with mechanical behavior of composite specimen.

very promising and piezo-resistive flexible sensor was responding very well to the mechanical change in the composite specimen.

8. Conclusions

In this study, a flexible strain sensor was fabricated using the electroplating process. The coating was carried out on nylon yarn, and it appeared thin and uniform. Then, the strain sensor was characterized and tested experimentally, and its behavior verified numerically. The results were very encouraging and reproducible. Next, the yarn sensor was incorporated into a composite material and standardized specimens were prepared and tested. The signal from the sensor was correlated perfectly with the local stress-signal of the composite panel. The following conclusions are drawn from this study:

- It confirmed the feasibility of fabricating a flexible strain sensor. The sensor was made of nylon yarn, coated with silver. The resistivity change was recorded in the elastic-plastic region, which showed that these flexible strain sensor wires can be used for SHM in different structures and can sense deformation or damage prior to failure.
- Numerical results verified damage behavior, that is, ductile failure and flaking off of coating as seen in experimentally fractured samples.
- It was found that the incorporation of these sensor wires would not affect the structural integrity of the specimen.

IntechOpen

Author details

Yumna Qureshi¹, Mostapha Tarfaoui^{1,2*}, Khalil K. Lafdi³ and Khalid Lafdi²

1 ENSTA Bretagne, IRDL-FRE CNRS 3744, Brest, France

2 University of Dayton, Dayton, OH, United States

3 Ohio Connections Academy, Mason, Ohio, United States

*Address all correspondence to: mostapha.tarfaoui@ensta-bretagne.fr

IntechOpen

© 2019 The Author(s). Licensee IntechOpen. This chapter is distributed under the terms of the Creative Commons Attribution License (<http://creativecommons.org/licenses/by/3.0>), which permits unrestricted use, distribution, and reproduction in any medium, provided the original work is properly cited. 

References

- [1] Campbell CF. Structural Composite Materials. Ohio: ASM International; 2010
- [2] El Moumen A, Tarfaoui M, Lafdi K, Benyahia H. Dynamic properties of carbon nanotubes reinforced carbon fibers/epoxy textile composites under low velocity impact. *Composites Part B: Engineering*. 2017;**125**(1–8)
- [3] Tarfaoui M. Experimental investigation of dynamic compression and damage kinetics of glass/epoxy laminated composites under high strain rate compression. *Advances in Composite Materials-Ecodesign and Analysis*. 2011
- [4] Nachtane M, Tarfaoui M, El Moumen A, Saifaoui D. Damage prediction of horizontal axis marine current turbines under hydrodynamic, hydrostatic and impacts loads. *Composite Structures*. 2017;**170**:146-157
- [5] Shah OR, Tarfaoui M. Determination of mode I & II strain energy release rates in composite foam core sandwiches: An experimental study of the composite foam core interfacial fracture resistance. *Composites Part B: Engineering*. 2017;**111**:134-142
- [6] El Moumen A, Tarfaoui M, Hassoon O, Lafdi K, Benyahia H, Nachtane M. Experimental study and numerical modelling of low velocity impact on laminated composite reinforced with thin film made of carbon nanotubes. *Applied Composite Materials*. 2018;**25**(2):309-320
- [7] ASM Handbook, Volume 21: Composites. ASM International; 2001
- [8] Awad ZK, Aravinthan T, Zhug Y, Gonzalez F. A review of optimization techniques used in the design of fibre composite structures for civil engineering applications. *Materials and Design*. 2012;**33**:534-544
- [9] Tarfaoui M, El Moumen A, Lafdi K. Progressive damage modeling in carbon fibers/carbon nanotubes reinforced polymer composites. *Composites Part B: Engineering*. 2017;**112**:185-195
- [10] Arbaoui J, Tarfaoui M, Bouery C, El Malki Alaoui A. Comparative study of mechanical properties and damage kinetics of two- and three-dimensional woven composites under high-strain rate dynamic compressive loading. *International Journal of Damage Mechanics*. 2016;**25**(6):878-899
- [11] Arbaoui J, Tarfaoui M, Arbaoui J, El Malki Alaoui A. Mechanical behavior and damage kinetics of woven E-glass/vinylester laminate composites under high strain rate dynamic compressive loading: Experimental and numerical investigation. *International Journal of Impact Engineering*. 2016;**87**:44-54
- [12] Ihn JB, Chang FK. Pitch-catch active sensing methods in structural health monitoring for aircraft structures. *Structural Health Monitoring*. 2008;**7**(1):5-19
- [13] Lynch JP, Law KH, Kiremidjian AS, Kenny TW, Carryer E, Partridge A. The design of a wireless sensing unit for structural health monitoring. In: 3rd International Workshop on Structural Health Monitoring; Stanford, CA; 2001
- [14] Yuan FG. *Structural Health Monitoring (SHM) in Aerospace Structures*. UK: Oxford, Elsevier; 2016
- [15] Michaels JE. Detection, localization and characterization of damage in plates with an in situ array of spatially distributed ultrasonic sensors. *Smart Materials and Structures*. 2008;**17**(3)

- [16] Zhu XP, Rizzo P, Marzani A, Bruck J. Ultrasonic guided waves for nondestructive evaluation/structural health monitoring of trusses. *Measurement Science and Technology*. 2010;21(4)
- [17] Sassi S, Tarfaoui M, Ben Yahia H. In-situ heat dissipation monitoring in adhesively bonded composite joints under dynamic compression loading using SHPB. *Composites Part B: Engineering*. 2018;54:64-76
- [18] Tarfaoui M, El Moumen A, Ben Yahia H. Damage detection versus heat dissipation in E-glass/epoxy laminated composites under dynamic compression at high strain rate. *Composite Structures*. 2018;186:50-61. DOI: 10.1016/j.compstruct.2017.11.083
- [19] Loayssa A. Optical fiber sensors for structural health monitoring. In: Mukhopadhyay SC, editor. *New Developments in Sensing Technology for Structural Health Monitoring*. Berlin, Heidelberg; 2011. pp. 335-358
- [20] Lin B, Giurgiutiu V. Modeling and testing of PZT and PVDF piezoelectric wafer active sensors. *Smart Materials and Structures*. 2006;15(4):1085-1093
- [21] Raghavan A, Cesnik CES. Review of guided-wave structural health monitoring. *The Shock and Vibration Digest*. 2007;39(2):91-114
- [22] Zilberstein V, Walrath K, Grundy D, Schlicker D, Goldfine N, Abramovici E, et al. MWM eddy-current arrays for crack initiation and growth monitoring. *International Journal of Fatigue*. 2003; 25(9-11):1147-1155
- [23] Speckmann H, Henrich R. Structural health monitoring (SHM)—Overview on technologies under development. In: *Proceedings of 16th WCNDT; 2004*
- [24] Christian B. Next generation structural health monitoring and its integration into aircraft design. *International Journal of Systems Science*. 2000;31(11):1333-1349
- [25] Varadan VK, Varadan V. Microsensors, microelectromechanical systems (mems), and electronics for smart structures and systems. *Smart Materials and Structures*. 2000;9(6): 953-972
- [26] Trifigny N, Kelly FM, Cochrane C, Boussu F, Koncar V, Soulat D. PEDOT: PSS-based piezo-resistive sensors applied to reinforcement glass fibres for in situ measurement during the composite material weaving process. *Sensors*. 2013;13(8):10749-10764
- [27] Atalay O, Kennon WR. Knitted strain sensors: Impact of design parameters on sensing properties. *Sensors*. 2014;14(3):4712-4730
- [28] Bashir T. Conjugated polymer-based conductive fibers for smart textile applications [Ph.D. Dissertation]. Sweden: Department of Chemical Engineering and Biotechnology, Chalmers University; 2013
- [29] Kaur G, Adhikari R, Cass P, Bown M, Gunatillake P. Electrically conductive polymers and composites for biomedical applications. *Royal Society of Chemistry Advances*. 2015;5:37553-37567
- [30] Djaja RG, Moses PJ, Carr AJ, Carnaby GA, Hankoff LD. Finite element modeling of an oriented assembly of continuous fibers. *Textile Research Journal*. 1992;62(8):445-457
- [31] Munro WA, Carnaby GA, Carr AJ, Moss PJ. Some textile applications of finite-element analysis. Part I: Finite elements for aligned fibre assemblies. *Journal of the Textile Institute*. 1997;88 (4):325-338
- [32] Munro WA, Carnaby GA, Carr AJ, Moss PJ. Some textile applications of

- finite-element analysis. Part II: Finite elements for yarn mechanics. *Journal of the Textile Institute*. 1997;**88**(4):339-351
- [33] He W, Wang X, Zhang S. Mechanical behavior of irregular fibers. Part II: Nonlinear tensile behavior. *Textile Research Journal*. 2001;**71**(11): 939-942
- [34] Keefe M, Edwards DC, Yang J. Solid modeling of yarn and fiber assemblies. *Journal of The Textile Institute*. 1992;**83** (2):185-196
- [35] Adanur S, Liao T. 3D modeling of textile composite preforms. *Composites Part B: Engineering*. 1998;**29**(6):787-793
- [36] Jiang Y, Chen X. Geometric and algebraic algorithms for modelling yarn in woven fabrics. *Journal of the Textile Institute*. 2005;**96**(4):237-245
- [37] Sriprateep K, Pattiya A. Computer aided geometric modeling of twist fiber. *Journal of Computer Science*. 2009;**5**(3): 221-225
- [38] Vassiliadis S, Kallivretaki A, Provatidis C. Mechanical modelling of multifilament twisted yarns. *Fibers and Polymers*. 2010;**11**(1):89-96
- [39] Peirce FT. Tensile tests for cotton yarns. V.—The weakest link theorems on the strength of long and of composite specimens. *Journal of the Textile Institute Transactions*. 1925;**17**(7):T355-T368
- [40] Hearle JWS, Grosberg P, Backer S. *Structural Mechanics of Fibers, Yarns, and Fabrics*. New York: John Wiley & Sons Inc; 1969
- [41] Treloar LRG, Riding G. Theory of the stress-strain properties of continuous-filament yarns. *Journal of the Textile Institute Transactions*. 1963; **54**:T156-T170
- [42] Riding G, Wilson N. The stress-strain properties of continuous-filament yarns. *Journal of the Textile Institute Transactions*. 1965;**56**(4):T205-T214
- [43] Liu T, Choi KF, Yuan L. Mechanical modeling of singles yarn. *Textile Research Journal*. 2007;**77**:123-130
- [44] Cartraud P, Messenger T. Computational homogenization of periodic beam-like structures. *International Journal of Solids and Structures*. 2006;**43**(3-4):686-696
- [45] Lee JH, Kim NR, Kim BJ, Joo YC. Improved mechanical performance of solution-processed MWCNT/Ag nanoparticle composite films with oxygen-pressure-controlled annealing. *Carbon*. 2012;**50**:98-106